Approximate entropy and auto mutual information analysis of the electroencephalogram in Alzheimer's disease patients

APPROXIMATE ENTROPY AND AUTO MUTUAL INFORMATION ANALYSIS OF THE ELECTROENCEPHALOGRAM IN ALZHEIMER'S DISEASE PATIENTS

D. Abásolo[1], J. Escudero[1], R. Hornero[1], C. Gómez[1] and P. Espino[2]

[1]*Biomedical Engineering Group, E.T.S. Ingenieros de Telecomunicación, University of Valladolid, Camino del Cementerio s/n, 47011, Valladolid (Spain)*

Phone: +34983423981

Fax: +34983423667

E-mail: danaba@tel.uva.es

Website: http://www.gib.tel.uva.es

[2]*Hospital Clínico San Carlos, c/Profesor Lagos s/n, 28040, Madrid (Spain)*

Corresponding author: D. Abásolo

Biomedical Engineering Group

E.T.S. Ingenieros de Telecomunicación, University of Valladolid, Camino del Cementerio s/n

47011

Valladolid (Spain)

Phone: +34983423981

Fax: +34983423667

Number of words of the manuscript (including title, affiliations, abstract, keywords, abbreviations and the whole manuscript, excluding the references, tables and figures captions): 5141
Number of words of the Abstract: 150

Abstract

We analysed the electroencephalogram (EEG) from Alzheimer's disease (AD) patients with two non-linear methods: Approximate Entropy (*ApEn*) and Auto Mutual Information (*AMI*). *ApEn* quantifies regularity in data, while *AMI* detects linear and non-linear dependencies in time series. EEGs from 11 AD patients and 11 age-matched controls were analysed. *ApEn* was significantly lower in AD patients at electrodes O1, O2, P3 and P4 ($p < 0.01$). The EEG *AMI* decreased more slowly with time delays in patients than in controls, with significant differences at electrodes T5, T6, O1, O2, P3 and P4 ($p < 0.01$). The strong correlation between results from both methods shows that the *AMI* rate of decrease can be used to estimate the regularity in time series. Our work suggests that non-linear EEG analysis may contribute to increase the insight into brain dysfunction in AD, especially when different time scales are inspected, as is the case with *AMI*.

Keywords: Alzheimer's disease, electroencephalogram, approximate entropy, mutual information, non-linear analysis.

AD: Alzheimer's disease; AMI: Auto mutual information; ApEn: Approximate entropy; AUC: Area under the ROC curve; CMI: Cross mutual information; D_2: Correlation dimension; EEG: Electroencephalogram; L1: Largest Lyapunov exponent; LZ: Lempel-Ziv; MI: Mutual information; MMSE: Mini-mental state examination; MSE: Multiscale entropy; ROC: Receiver operating characteristic; SampEn: Sample entropy; SD: standard deviation

Introduction

Alzheimer's disease (AD) is a primary neurodegenerative disorder of unknown aetiology that gradually destroys brain cells and represents the most prevalent form of dementia in western countries [7]. AD is characterized by progressive impairments in cognition and memory whose course lasts several years prior to the death of the patient [23]. These clinical features are accompanied by histological changes in the brain, which include widespread cortical atrophy, intracellular deposition of neurofibrillary tangles and extracellular deposition of senile plaques, particularly in the hippocampus and the cerebral cortex [43]. Although a definite diagnosis is only possible by necropsy [42], a differential diagnosis with other types of dementia and with major depression should be attempted. Magnetic resonance imaging and computerized tomography can be normal in the early stages of AD but a diffuse cortical atrophy is the main sign in brain scans. Mental status tests are also useful.

In order to improve quality diagnosis, electrical brain activity has been widely analysed using electroencephalogram (EEG) recordings. The EEG has proved to be useful in the characterization of different physiological or pathological conditions, such as, for example, sleep [29] or epilepsy [11], [18]. Particularly, the EEG has been used as a tool for diagnosing dementias for several decades. Several reasons explain why intensive research has been performed on the EEG in AD.

One reason is that AD is a cortical dementia in which EEG abnormalities are more frequently shown. Furthermore, coherence analysis of the EEG in AD allows non-invasive assessment of synaptic dysfunction [23]. In general, AD patients' EEGs are characterized by a shift of the power spectrum to lower frequencies and a coherence decrease among cortical areas [23], although in the early stages of the disease the EEG may exhibit normal frequencies [28].

Non-linearity in the brain is introduced even at the neuronal level [5], since the dynamical behaviour of individual neurons is governed by threshold and saturation phenomena. Given the highly non-linear nature of the neuronal interactions at multiple levels of temporal and spatial scales, the EEG appears to be an appropriate area for non-linear time series analysis [26]. Furthermore, recent progress in the theory of non-linear dynamics has provided new methods to study the EEG [23], [45]. The investigations of the electrical brain activity have revealed possible medical applications, since analysis based on non-linear dynamics yields information unavailable using traditional EEG spectral-band analysis [39]. Moreover, it has been shown that non-linear analysis is useful to characterize the EEG in different pathological states like epilepsy [27], schizophrenia [41], or the Creutzfeldt-Jakob [6] and Parkinson's diseases [44]. This has given rise to the possibility that the underlying mechanisms of the brain function may be explained in a more appropriate way by non-linear dynamics. A detailed review of the state of the art in EEG analysis with non-linear techniques can be found in [45].

Several authors have analysed the EEG in AD patients with non-linear methods. It has been shown that AD patients have lower correlation dimension (D_2) values – a measure of the underlying system dimensional complexity – than control subjects [24], [39]. Furthermore, AD patients also have significantly lower values of the largest Lyapunov exponent ($L1$) – a metric that can be interpreted as a measure of the dynamical state of neuronal networks of the brain [41] – than controls in almost all EEG channels [24]. However, estimating the non-linear dynamical complexity of physiological time series using measures such as D_2 and $L1$ is problematic, as the amount of data required for meaningful results in their computation is usually beyond the experimental possibilities [12]. Thus, the study of the EEG background activity with more suitable non-linear methods becomes necessary.

The present study was undertaken to examine the EEG background activity in AD with two non-linear methods: approximate entropy (*ApEn*) and auto mutual information (*AMI*). *ApEn* is a family of statistics introduced to provide a widely applicable, statistically valid formula that will

distinguish data sets by a measure of regularity [33]. Preliminary evidence has shown its usefulness in different EEG studies [8], [40]. On the other hand, the mutual information (*MI*) provides a measure of both linear and non-linear statistical dependencies between two time series [25]. Applied to the EEG, *MI* has been used to describe the information transmission in the brain in different states [30], [48], to extract characterizing features in epileptic seizures [46] and to predict the response to anaesthesia [22]. In particular, the *AMI* – i.e. the *MI* between a time series and a delayed version of itself – can be useful in the characterization of a signal [25]. In this pilot study, we wanted to test the hypothesis that the non-linear characteristics of the EEG background activity in AD patients' EEG would be different from those of age-matched controls, hence indicating an abnormal type of dynamics. Furthermore, we evaluated the possible correlation between the results obtained with both non-linear methods. Finally, we compared results with those obtained using other non-linear methods and the same database in previous works.

Material and Methods

Subjects and EEG recording

Twenty-two subjects participated in this study. Eleven patients (5 men and 6 women; age = 72.5 ± 8.3 years, mean ± standard deviation SD) fulfilling the criteria of probable AD were recruited from the Alzheimer's Patients' Relatives Association of Valladolid and referred to the University Hospital of Valladolid (Spain), where the EEG was recorded. All of them had undergone a thorough clinical evaluation that included clinical history, physical and neurological examinations and brain scans. Mini-Mental State Examination (MMSE) [14] was used to assess the cognitive function. The mean MMSE score for the patients was 13.1 ± 5.9 (Mean ± SD). Five of them had a score of less than 12 points, indicating a severe degree of dementia.

The control group consisted of 11 age-matched control subjects without past or present neurological disorders (7 men and 4 women; age = 72.8 ± 6.1 years, mean ± SD). The MMSE score value was 30 for all control subjects. Informed consent was obtained from all control subjects and all caregivers of the demented patients. The study was approved by the local ethics committee.

More than five minutes of EEG data from each subject were recorded with a Profile Study Room 2.3.411 EEG equipment (Oxford Instruments) at electrodes F3, F4, F7, F8, Fp1, Fp2, T3, T4, T5, T6, C3, C4, P3, P4, O1, O2, Fz, Cz and Pz of the international 10-20 system with linked

ear lobes reference. The sampling frequency was 256 Hz, with a 12-bit A-to-D precision. The EEG background activity from all control subjects and AD patients was recorded while they were awake, at rest and with their eyes closed and under vigilance control. All the traces from the control group showed a posterior alpha rhythm except two cases in which the EEGs were desynchronized. The patients' EEGs showed a posterior alpha rhythm in the normal range or a slower rhythm (8-Hz alpha rhythm or theta-range activity) depending on the slowing of the tracing. In no case electroencephalographic signs of sleep were recorded.

All EEG background activity recordings were visually inspected by a specialist physician to check for eye movement and other artefacts. Thus, only EEG data free from electro-oculographic and movement artefacts and with minimal electromyographic (EMG) activity were selected for non-linear analysis. Afterwards, EEGs were organized in 5 second artefact-free epochs (1280 points) and were copied as ASCII files for off-line analysis on a personal computer. An average number of 30.0 ± 12.4 artefact-free epochs (Mean ± SD) were selected from each electrode and each subject. Furthermore, all recordings were digitally filtered with a Hamming window finite impulse response band-pass filter of 425th order with cut-off frequencies at 0.5 Hz and at 40 Hz, designed with Matlab®. The attenuation at the cut-off frequencies was fixed at 6 dB and all frequencies above 42Hz were attenuated more than 60 dB. The cut-off frequencies were chosen to remove the residual EMG activity and the noise owing to the electrical mains.

Approximate entropy (*ApEn*)

ApEn is a family of statistics recently introduced as a quantification of regularity in the data without any *a priori* knowledge about the system generating them [35]. It was constructed by Pincus [33], motivated by applications to short and noisy data sets, along with thematically similar lines to the Kolmogorov-Sinai entropy. However, the focus was different: to provide a widely applicable, statistically valid formula that will distinguish data sets by a measure of regularity [33]. *ApEn* is scale invariant and model independent and it discriminates series for which clear feature recognition is difficult [34]. Notably, it detects changes in underlying episodic behaviour not reflected in peak occurrences or amplitudes [36]. Moreover, *ApEn* can be applied to short time series and is finite for stochastic, noisy deterministic and composite processes [34].

ApEn assigns a non-negative number to a time series, with larger values corresponding to more irregularity in the data. Two input parameters, a run length m and a tolerance window r, must be specified. Briefly, *ApEn* measures the logarithmic likelihood that runs of patterns that are close

(within r) for m contiguous observations remain close (within the same tolerance width r) on subsequent incremental comparisons. *ApEn*(m, r, N), where N is the number of points of the time series, must be considered a family of characterizing measures: comparisons between time series can only be made with the same values of m, r and N [34].

Formally, given N data points from a time series $\{x(n)\} = x(1), x(2), \ldots, x(N)$, one should follow these steps to compute *ApEn* [34]:

1. Form $N–m+1$ vectors $X(1)\ldots X(N–m+1)$ defined by: $X(i) = [x(i), x(i+1),\ldots, x(i+m–1)]$, $i = 1\ldots N–m+1$.
2. Define the distance between $X(i)$ and $X(j)$, $d[X(i),X(j)]$, as the maximum absolute difference between their respective scalar components, i.e. the maximum norm:

$$d[X(i),X(j)] = \max_{k=1,2,\ldots m} |x(i+k-1)-x(j+k-1)| . \quad (1)$$

3. For a given $X(i)$, count the number of j ($j = 1\ldots N–m+1$) so that $d[X(i), X(j)] \le r$, denoted as $N^m(i)$. Then, for $i = 1\ldots N–m+1$,

$$C_r^m(i) = N^m(i)/(N-m+1) . \quad (2)$$

4. Compute the natural logarithm of each $C_r^m(i)$, and average it over i,

$$\phi^m(r) = \frac{1}{N-m+1}\sum_{i=1}^{N-m+1} \ln C_r^m(i) . \quad (3)$$

5. Increase the dimension to $m+1$. Repeat steps 1) to 4) and find $C_r^{m+1}(i)$ and $\phi^{m+1}(r)$
6. Theoretically, *ApEn* is defined as:

$$ApEn(m,r) = \lim_{N\to\infty}\left[\phi^m(r)-\phi^{m+1}(r)\right] \quad (4)$$

7. In practice, the number of data points N is finite. We implement this formula by defining the statistic [33]:

$$ApEn(m,r,N) = \phi^m(r)-\phi^{m+1}(r) . \quad (5)$$

ApEn has been used to characterize different biomedical signals [34]. In particular, it discriminates atypical EEGs [8] from normative counterparts. The possible usefulness of *ApEn* in epileptic seizure prediction has been suggested [40], but this claim has yet to be validated. Furthermore, *ApEn* has been used to quantify the depth of anaesthesia [49].

Although m and r are critical in determining the outcome of *ApEn*, no guidelines exist for optimising their values. In principle, the accuracy and confidence of the entropy estimate improve as the number of matches of length m and $m + 1$ increases. This can be done by choosing small m (short templates) and large r (wide tolerance). However, there are penalties for criteria that are too

relaxed [33]. It has been suggested to estimate *ApEn* with parameter values of m = 1 and 2, and r = 0.1, 0.15, 0.2 and 0.25 times the SD of the original data sequence $\{x(n)\}$ [34]. Normalizing r in this manner gives *ApEn* a translation and scale invariance; in this way it remains unchanged under uniform process magnification, reduction, or constant shift to higher or lower values [34]. Furthermore, it has been demonstrated that these input parameters produce good statistical reproducibility for *ApEn* for time series of length $N \geq 60$, as considered herein [33], [35]. In this pilot study, *ApEn* was estimated with m = 1 and r = 0.25 times the SD of the original data sequence. In this way we selected a small m value and a large r value to improve the accuracy of the entropy estimate within the limits that produce good statistical reproducibility for *ApEn*.

Auto mutual information (*AMI*)

MI is a metric derived from Shannon's information theory to estimate the information gained from observations of one random event on another [15], [38], [47]. *MI* measures both linear and non-linear dependences between two time series [15], [38]. Hence, it can be regarded as a non-linear equivalent of the correlation function [20], [38]. Similarly to this linear statistic, *MI* can be applied to time-delayed versions of the same sequence – *AMI* – or to two different signals – cross mutual information function (*CMI*) – [25].

In general, the *MI* between two measurement x_i and y_i is the amount of information that the former provides about the latter. Thus, the *AMI* estimates, on average, the degree to which $x(t+\tau)$ can be predicted from $x(t)$ [15], [25], [31]. The *AMI* between $x(t)$ and $x(t+\tau)$ is [25]:

$$I_{XX_\tau} = \sum_{x(t),x(t+\tau)} P_{XX_\tau}[x(t),x(t+\tau)] \cdot \log_2 \left\{ \frac{P_{XX_\tau}[x(t),x(t+\tau)]}{P_X[x(t)] \cdot P_{X_\tau}[x(t+\tau)]} \right\}. \qquad (6)$$

$P_X[x(t)]$ is the probability density for the measurement $x(t)$, while $P_{XX_\tau}[x(t),x(t+\tau)]$ is the joint probability density for the measurements of $x(t)$ and $x(t+\tau)$.

It has been shown that the *AMI* rate of decrease with increasing time delays is correlated with the signal entropy [32], [37]. This fact has been used to characterize the EEG [25] and magnetoencephalogram (MEG) recordings [17] from AD patients in comparison with control subjects. This parameter was also applied to EEG signals from schizophrenic patients [30].

In this pilot study, the *AMI* was estimated over a time delay from 0 to 0.5 s and was normalized so that $AMI(\tau = 0) = 1$. The *AMI* is based on the amplitude distributions of $x(t)$ on different time

scales [10]. These distributions are estimated from histograms [4], [25]. For a fixed sequence length, if larger sampling bins are used to construct the histograms, the estimations of the average probabilities are more accurate. However, the joint probability distribution could be too flat and the *MI* could be underestimated. On the other hand, smaller partitions may enhance the changes in the joint probability distribution over short distances, but they produce fluctuations due to the small sample size. Thus, *MI* could be overestimated [25]. In this study, we used 12 bins to construct the histograms, which provided stable estimates and is similar to the number of bins that would be obtained using the criteria suggested in [10]. The probability densities in (Eq. 6) were estimated as follows:

- Histograms of the signal $x(t)$ and its time-delayed version $x(t+\tau)$ were constructed.
- Probability distributions of $x(t)$ and $x(t+\tau)$ were obtained as the ratio between the number of samples in each of the 12 bins and the total number of samples.
- To calculate the joint probability distribution, the $(x(t), x(t+\tau))$ plane was partitioned into a 12x12 matrix. The joint probability density was obtained dividing the number of samples in each cell of the aforementioned plane by the total number of samples.

The *AMI* rate of decrease was estimated using a least-squares fitting method assuming a first-order monomial, $y = ax + 1$, where x denotes the time delay (measured in seconds) and y is the *AMI* curve. This rate of decrease (a) was calculated from a time delay 0 to the first relative minimum value, located as the point where the difference between the current sample and the previous one becomes non-negative. Therefore, different time scales were simultaneously taken into account when characterizing the signal. This methodology can be useful when no information is given in advance about the prominent time scales of a time series [20], [21], [31]. Furthermore, this decrease rate is correlated with the signal entropy [32]. Consequently, this variable can be considered a signal irregularity estimator and be used as a characterizing feature of the EEG.

Statistical analysis

Student's *t*-test was used to evaluate the statistical differences between the *ApEn* values and the *AMI* rates of decrease for AD patients and control subjects. Differences were considered statistically significant if the p value was lower than 0.01. Normality of the data distribution was assessed with the Kolmogorv-Smirnov test, whereas homoscedasticity was analysed with Levene's

test. Furthermore, the relationship between the *AMI* rate of decrease and *ApEn* was examined with Pearson's linear correlation coefficient (ρ).

Finally, the ability to discriminate AD patients from control subjects at the electrodes where $p < 0.01$ was evaluated using Receiver Operating Characteristic (ROC) curves [50]. We define the sensitivity as the rate of patients with a diagnosis of AD who test positive (i.e. the true positive rate), whereas the specificity represents the fraction of controls correctly recognized (i.e. the true negative rate). Accuracy is a related parameter that quantifies the total number of subjects (AD patients and control subjects) precisely classified. We set the optimum threshold as the cut-off point in which the highest accuracy (minimal false negative and false positive results) was obtained.

Results

ApEn was estimated for channels F3, F4, F7, F8, Fp1, Fp2, T3, T4, T5, T6, C3, C4, P3, P4, O1 and O2 with $m = 1$ and $r = 0.25$ times the SD of the original data sequence. The results are summarized in Table 1. It can be seen that *ApEn* was lower in AD patients than in control subjects at 15 electrodes, with significant differences between both groups ($p < 0.01$) at P3, P4, O1 and O2. These results suggest that the EEG activity of AD patients is more regular than in the control subjects' brain.

INSERT TABLE 1 AROUND HERE

The normalized *AMI* curves of the control subjects and AD patients decrease with increasing values of the time delay for all subjects at all electrodes. Then, *AMI* curves show a transitory oscillation which decays as τ increases [25]. As an example of this characteristic, Figure 1(a) depicts the normalized *AMI* curves for two of these profiles, one obtained from an AD patient's EEG epoch and other from a control subject's one. Additionally, Figure 1(b) represents the average *AMI* curves of the control subjects and AD patients at electrode O2. Both profiles decrease gradually with increasing values of the time delay. In order to estimate the *AMI* rate of decrease, relative minimum values were located between the decreasing slope and the oscillations for each *AMI* curve obtained from every EEG epoch. The mean *AMI* rates of decrease for all electrodes are summarized in Table 2. These results show that, with the exception of electrode T4, the *AMI*

decreases more slowly in AD patients, with significant differences ($p < 0.01$) at T5, T6, P3, P4, O1 and O2.

INSERT FIGURE 1 – IT CONSISTS OF TWO FIGURES: FIGURE 1(a) AND FIGURE 1(b) – AND TABLE 2 AROUND HERE

We evaluated the ability of both methods to discriminate AD patients from control subjects at the electrodes where significant differences were found using ROC plots. The sensitivity, specificity and accuracy values are shown in Table 3, where the optimum thresholds to achieve these values are also included. Accuracies were higher using the *AMI* rate of decrease, with values over 80% at the six electrodes were $p < 0.01$, reaching 90.91% at P3. On the other hand, the accuracies achieved with *ApEn* were always inferior to 80%. Furthermore, we evaluated the area under the ROC curve (AUC), as this parameter can be roughly used to classify the precision of a diagnostic test. The value for the AUC can be interpreted as follows: an area of 0.9339 (obtained with the *AMI* rate of decrease at electrode P3, for example) means that a randomly selected individual from the control subjects' group has an *AMI* rate of decrease value smaller – i.e. more negative, meaning a faster decrease of the *AMI* curves – than that of a randomly chosen individual from the AD patients' group in 93.39% of the time [50]. However, from Table 3 it seems that the accuracy differences between *ApEn* and the *AMI* rate of decrease do not correspond to important changes in the AUC.

Finally, we examined the correlation between the *ApEn* values and the *AMI* rates of decrease. Our results show a strong correlation between both metrics, with $\rho < -0.86$ for all electrodes ($p << 0.01$). The negative correlation index is due to the nature of the *AMI* rates of decrease, where a more negative value is associated with higher irregularity, while *ApEn* assigns smaller values to more regular time series. Figure 2 represents the *ApEn* values vs. the *AMI* rates of decrease at electrode P3 for control subjects and AD patients.

INSERT FIGURE 2 AROUND HERE

Discussion and conclusions

In this pilot study, we analysed the EEG background activity of 11 AD patients and 11 control subjects with *ApEn* and *AMI*. *ApEn* is a family of statistics that quantifies the regularity in time series, with increasing values corresponding to more irregularity [34]. *AMI* estimates the degree to which $x(t+\tau)$ can be predicted from $x(t)$ [25]. Moreover, the *AMI* rate of decrease with increasing τ can be used to characterize a time series [25]. Both methods do not require a large number of data points to be reliably estimated [25], [34]. Particularly, estimating *ApEn* with $m = 1$ and $r = 0.25$ times the SD of the data produces good statistical reproducibility for time series of length $N \geq 60$, as considered herein [33], [35]. Thus, both metrics are much better suited for EEG analysis than traditional non-linear techniques such as $L1$ or D_2.

We found that *ApEn* was significantly lower in the AD patients' EEG at electrodes P3, P4, O1 and O2 ($p < 0.01$). Furthermore, our study shows that the *AMI* decreases more slowly with τ in AD patients. We estimated the *AMI* rate of decrease to characterize the EEG, and we found significant differences between both groups at electrodes T5, T6, P3, P4, O1 and O2 ($p < 0.01$). Some authors have chosen the *AMI* rate of decrease to quantify complexity in time series [25]. Our study reveals that the values of the *AMI* rate of decrease are strongly correlated with *ApEn*, something that could be expected [32], [37]. Given the fact that *ApEn* is a regularity estimator, the strong correlation between both metrics indicates that the *AMI* rate of decrease can be used to quantify the regularity of a time series instead of its complexity, as some authors have previously suggested [25]. A complexity measure should vanish for both completely regular and completely random system [9], something that does not happen with *ApEn* [19]. Moreover, a steeper decline of the *AMI* for a given time series does not necessarily point out that physiologic or physical complexity has increased, as it may be related to a breakdown in multiscale correlations or to more subtle alterations in non-linear control [16]. The negative relationship in the correlation between both metrics (as shown in Figure 2) is due to the fact that, while *ApEn* values are positive and larger in more irregular time series, the more negative *AMI* rates of decrease are associated with higher irregularity.

We also evaluated the diagnostic accuracy of both methods with ROC curves. The *AMI* rate of decrease provided a more accurate classification than *ApEn*, with values over 80% at all electrodes where significant differences between AD patients and control subjects were found. This suggests

that, although both metrics are strongly correlated, the *AMI* rate of decrease might be more useful to differentiate AD patients from elderly control subjects.

We have previously analysed the same EEG dataset with other non-linear techniques, such as sample entropy (*SampEn*) [2], Lempel-Ziv (*LZ*) complexity [3] or multiscale entropy (*MSE*) [13]. A detailed description of these metrics can be found in the previous references. Basically, *SampEn* is a family of statistics closely related to *ApEn* introduced to quantify the regularity of a time series and to reduce the *ApEn* bias. With parameter values m =1 and r = 0.25 times the SD of the data, we found that AD patients have significantly lower *SampEn* values than control subjects at electrodes O1, O2, P3 and P4 ($p < 0.01$) [2]. *LZ* complexity is a non-parametric measure of complexity in a one-dimensional signal related to the number of distinct substrings and the rate of their recurrence. The signal must be transformed into a finite symbol sequence before calculating the *LZ* complexity value. Our results suggested that a three symbol conversion might give more detailed insight into the differences between the AD patients and control subjects' EEGs than a binary conversion [3]. Particularly, we found a significantly reduced *LZ* complexity ($p < 0.01$) at electrodes T5, P3, P4 and O1 in AD patients. [3]. Finally, *MSE* is a measure of complexity based on the analysis of the original signal on different temporal scales. It is based on successive computations of *SampEn* on coarse-grained sequences, each of which represents the system dynamics on a different time scale. The *MSE* was estimated with m = 1, r = 0.25 times the SD of the original time series and a maximum time scale ε_{MAX} = 12. The analysis of our AD patients and control subjects' database with *MSE* showed important differences in the shape of the *MSE* profiles on the larger time scales, with significant differences at electrodes F3, F7, Fp1, Fp2, T5, T6, P3, P4, O1 and O2 ($p < 0.01$) [13]. All these techniques can be applied to relatively short and noisy time series, irrespective of whether their origin is stochastic or deterministic. Table 3 summarizes the test results for *ApEn*, the *AMI* rate of decrease, *SampEn*, *LZ* complexity and *MSE*.

INSERT TABLE 3 AROUND HERE

As expected, results with *SampEn* and *ApEn* were similar due to the relation between both metrics. However, the accuracy was slightly lower with *ApEn* than with *SampEn* at electrode P4 [2]. Accuracies reached 81.82% at 3 electrodes with *LZ* complexity, improving the results obtained with *ApEn* [3]. On the other hand, the inspection of EEG signals with *MSE* revealed their complex

structure [13]. As the *MSE* profile values are higher in control subjects than in AD patients for most scales, it can be concluded that EEG background activity is less complex in patients, something that is also in agreement with our *LZ* complexity results [13]. Furthermore, the *MSE* profile slope for large time scales in AD patients is significantly different than in control subjects at 10 electrodes while *LZ* complexity only showed them at 4 electrodes. A possible explanation for this result might be that the inspection of different time scales provides an advantage in comparison to the use of other non-linear measures based on one time scale only when analysing physiological signals [9], [20], [31]. In addition, the comparison of results obtained with the *AMI* rates of decrease and other non-linear regularity metrics, like *ApEn* and *SampEn*, substantiates this claim. Furthermore, the classification accuracies obtained with the slope of the *MSE* profiles or the *AMI* rates of decrease are generally higher than using *ApEn*, *SampEn* or *LZ* complexity. This suggests that the analysis of different time scales could provide additional information that may improve AD diagnosis. On the other hand, both *MSE* and *AMI* results are based on the estimation of characteristics from graphical representations (i.e. slopes in plots), while *ApEn*, *SampEn* and *LZ* complexity results are directly obtained from the EEG time series.

Our results are consistent with previous studies showing changes in the EEG of AD patients in comparison to age-matched control subjects with different non-linear metrics [1], [24], [25], [39], [44]. The abnormalities in the AD patients' EEG could be explained by a change of the dynamics in the brain. However, the implications of this EEG changes are not clear. Among others, three mechanisms can be responsible for it: neuronal death, a general effect of neurotransmitter deficiency and loss of connectivity of local neural networks [23].

Some limitations of this pilot study must be mentioned. Firstly, the sample size was small. To prove the usefulness of these techniques as an AD diagnostic tool, this approach should be extended on a much larger patient population. Moreover, as physicians only make a diagnosis of AD with an accuracy of about 90%, the sample may not fully represent this disease. Moreover, the detected regularity increase in the EEG is not specific to AD and further work must be carried out to examine non-linear EEG activity in other types of dementia.

In summary, our findings show the possibility to analyse the dynamical behaviour of the brain in AD patients and to detect significant differences with *ApEn* and *AMI*. The strong correlation between results from both methods suggests that the *AMI* rate of decrease can be used to estimate the regularity in time series. Although these techniques cannot yet be applied as a diagnostic tool,

our results prove the potential applications of these methods in reflecting differences in the irregularity of EEG data time series of patients with a diagnosis of AD and control subjects. The decrease of the EEG regularity leads us to think that EEG analysis with *ApEn* and *AMI* could be a useful tool to increase our insight into brain dysfunction in this disease. Furthermore, the comparison of our results with those obtained using non-linear metrics based on just one time scale suggests that the analysis of different time scales with *AMI* might provide a better insight into the EEG background activity characteristics and the changes associated with AD. In addition, these methods could also be useful to characterize the EEG in other cerebral disorders like, for instance, Parkinson's disease, vascular dementia, epilepsy or schizophrenia.

Acknowledgments

This work was supported by grant projects VA102A06 and VA108A06 from Consejería de Educación de la Junta de Castilla y León and by a grant project from Ministerio de Educación y Ciencia and FEDER grant MTM 2005-08519-C02-01.

References

[1] Abásolo D, Hornero R, Espino P et al (2005) Analysis of regularity in the EEG background activity of Alzheimer's disease patients with Approximate Entropy. Clin Neurophysiol 116:1826–1834 DOI 10.1016/j.clinph.2005.04.001

[2] Abásolo D, Hornero R, Espino P et al (2006) Entropy analysis of the EEG background activity in Alzheimer's disease patients. Physiol Meas 27:241–253 DOI 10.1088/0967-3334/27/3/003

[3] Abásolo D, Hornero R, Gómez C et al (2006) Analysis of EEG background activity in Alzheimer's disease patients with Lempel-Ziv complexity and Central Tendency Measure. Med Eng Phys 28:315–322 DOI 10.1016/j.medengphy.2005.07.004

[4] Alonso J F, Mañanas M A, Hoyer D et al (2007) Evaluation of respiratory muscles activity by means of mutual information function at different levels of ventilatory effort. IEEE Trans Biomed Eng 54:1573–1582 DOI: 10.1109/TBME.2007.893494

[5] Andrzejak R G, Lehnertz K, Moormann F et al (2001) Indications of nonlinear deterministic and finite-dimensional structures in time series of brain electrical activity: Dependence on recording region and brain state. Phys Rev E 64:061907 DOI 10.1103/PhysRevE.64.061907

[6] Babloyantz A, Destexhe A (1988) The Creutzfeldt-Jakob disease in the hierarchy of chaotic attractors in From chemical to biological organization, Markus M, Müller S, Nicolis G, (Eds.) Springer-Verlag, Berlin 307–316

[7] Bird T D (2001) Alzheimer's disease and other primary dementias in Harrison's principles of internal medicine, Braunwald E, Fauci A S, Kasper D L et al (Eds), The McGraw-Hill Companies Inc, New York, NY 2391–2399

[8] Bruhn J, Röpcke H, Rehberg B et al (2000) Electroencephalogram approximate entropy correctly classifies the occurrence of burst suppression pattern as increasing anesthetic drug effect. Anesthesiology 93:981–985

[9] Costa M, Goldberger A L, Peng C K (2005) Multiscale entropy analysis of biological signals Phys Rev E 71:021906. DOI 10.1103/PhysRevE.71.021906

[10] David O, Cosmelli D, Friston K J (2004) Evaluation of different measures of functional connectivity using a neural mass model. Neuroimage 21:659–673 DOI 10.1016/j.neuroimage.2003.10.006

[11] De Lucia M, Fritschy J, Dayan P et al (2008) A novel method for automated classification of epileptiform activity in the human electroencephalogram-based on independent component analysis. Med Biol Eng Comput 46:263–272 DOI 10.1007/s11517-007-0289-4
[12] Eckmann J P, Ruelle D (1992) Fundamental limitations for estimating dimensions and Lyapunov exponents in dynamical systems. Physica D 56:185–187 DOI 10.1016/0167-2789(92)90023-G
[13] Escudero J, Abásolo D, Hornero R et al (2006) Analysis of electroencephalograms in Alzheimer's disease patients with multiscale entropy. Physiol Meas 27:1091–1106 DOI 10.1088/0967-3334/27/11/004
[14] Folstein M F, Folstein S E, McHugh P R (1975) Mini-mental state. A practical method for grading the cognitive state of patients for the clinician, J Psychiat Res 12:189-198 DOI 10.1016/0022-3956(75)90026-6
[15] Fraser A M, Swinney H L (1986) Independent coordinates for strange attractors from mutual information. Phys Rev A 33:1134–1140 DOI 10.1103/PhysRevA.33.1134
[16] Goldberger A L, Peng C K, Lipsitz L A (2002) What is physiologic complexity and how does it change with aging and disease? Neurobiol Aging 23:23–26 DOI 10.1016/S0197-4580(01)00266-4
[17] Gómez C, Hornero R, Abásolo D et al (2007) Analysis of the magnetoencephalogram background activity in Alzheimer's disease patients with auto mutual information. Comput Meth Prog Bio 87:239–247 DOI 10.1016/j.cmpb.2007.07.001
[18] Hesse C W, James C J (2007) Tracking and detection of epileptiform activity in multichannel ictal EEG using signal subspace correlation of seizure source scalp topographies. Med Bio Eng Comput 45:909–916 DOI 10.1007/s11517-006-0103-8
[19] Hornero R, Aboy M, Abásolo D et al (2005) Interpretation of approximate entropy: analysis of intracranial pressure approximate entropy during acute intracranial hypertension. IEEE Trans Biomed Eng 52:1671–1680 DOI 10.1109/TBME.2005.855722
[20] Hoyer D, Pompe B, Chon K H et al (2005) Mutual information function assesses autonomic information flow of heart rate dynamics at different time scales. IEEE Trans Biomed Eng 52:584–592 DOI 10.1109/TBME.2005.844023
[21] Hoyer D, Friedrich H, Frank B et al (2006) Autonomic information flow improves prognostic impact of task force HRV monitoring. Comput Meth Prog Bio 81:246–255 DOI 10.1016/j.cmpb.2006.01.002
[22] Huang L, Yu P, Ju F et al (2003) Prediction of response to incision using the mutual information of electroencephalogram during anaesthesia. Med Eng Phys 25:321–327 DOI 10.1016/S1350-4533(02)00249-7
[23] Jeong J (2004) EEG dynamics in patients with Alzheimer's disease. Clin Neurophysiol 115:1490–1505 DOI 10.1016/j.clinph.2004.01.001
[24] Jeong J, Chae J H, Kim S Y et al (2001) Nonlinear dynamic analysis of the EEG in patients with Alzheimer's disease and vascular dementia. J Clin Neurophysiol 18:58–67.
[25] Jeong J, Gore J C, Peterson B S (2001) Mutual information analysis of the EEG in patients with Alzheimer's disease. Clin Neurophysiol 112:827–835 DOI 10.1016/S1388-2457(01)00513-2
[26] Kantz H, Schreiber T (1997) Nonlinear Time Series Analysis. Cambridge University Press, Cambridge.
[27] Lehnertz K, Mormann F, Kreuz T et al (2003) Seizure prediction by nonlinear EEG analysis. IEEE Eng Med Biol 22:57–63 DOI 10.1109/MEMB.2003.1191451
[28] Markand O N (1990) Organic brain syndromes and dementias in Current Practice of Clinical Electroencephalography, Daly D D, Pedley T A (Eds), Raven Press, New York 401–423.
[29] Mendez M O, Bianchi A M, Montano N et al (2008) On arousal from sleep: time-frequency análisis. Med Biol Eng Comput 46:341–351 DOI 10.1007/s11517-008-0309-z
[30] Na S H, Jin S H, Kim S Y et al (2002) EEG in schizophrenic patients: mutual information analysis. Clin Neurophysiol 113:1954–1960 DOI 10.1016/S1388-2457(02)00197-9
[31] Palacios M, Friedrich H, Götze C et al (2007) Changes of autonomic information flow due to idiopathic dilated cardiomyopathy. Physiol Meas 28:677–688 DOI 10.1088/0967-3334/28/6/006
[32] Palus M (1996) Coarse-grained entropy rates for characterization of complex time series. Physica D 93:64–77 DOI 10.1016/0167-2789(95)00301-0
[33] Pincus S M (1991) Approximate entropy as a measure of system complexity. Proc Natl Acad Sci USA 88:2297–2301.

[34] Pincus S M (2001) Assessing serial irregularity and its implications for health. Ann NY Acad Sci 954:245–267.
[35] Pincus S M, Goldberger A L (1994) Physiological time series analysis: what does regularity quantify? Am J Physiol (Heart Circ Physiol) 266:H1643–H1656.
[36] Pincus S M, Keefe D L (1992) Quantification of hormone pulsatility via an approximate entropy algorithm. Am J Physiol (Endocrinol Metab) 262:E741–E754.
[37] Pompe B (1993) Measuring statistical dependencies in a time series. J Stat Phys 73:587–610 DOI 10.1007/BF01054341
[38] Pompe B, Blidh P, Hoyer D et al (1998) Using mutual information to measure coupling in the cardiorespiratory system. IEEE Eng Med Biol 17:32–39 DOI 10.1109/51.731318
[39] Pritchard W S, Duke D W, Coburn K L et al (1994) EEG-based neural-net predictive classification of Alzheimer's disease versus control subjects is augmented by non-linear EEG measures. Electroenceph Clin Neurophysiol 91:118–130 DOI 10.1016/0013-4694(94)90033-7
[40] Radhakrishnan N, Gangadhar B N (1998) Estimating regularity in epileptic seizure time-series data. A complexity-measure approach. IEEE Eng Med Biol 17:89–94 DOI 10.1109/51.677174
[41] Röschke J, Fell J, Beckmann P (1995) Non-linear analysis of sleep EEG data in schizophrenia: calculation of the principal Lyapunov exponent. Psychiatr Res 56:257–269 DOI 10.1016/0165-1781(95)02562-B
[42] Rossor M (2001) Alzheimer's disease in Brain's Diseases of the Nervous System, Donaghy M (Ed.) Oxford University Press, Oxford 750–754.
[43] Selkoe D J (1994) Cell biology of the amyloid beta-protein precursor and the mechanism of Alzheimer's disease. Annu Rev Cell Biol 10:373–403 DOI 10.1146/annurev.cb.10.110194.002105
[44] Stam C J, Jelles B, Achtereekte H A M et al (1995) Investigation of EEG non-linearity in dementia and Parkinson's disease. Electroenceph Clin Neurophysiol 95:309–317 DOI 10.1016/0013-4694(95)00147-Q
[45] Stam C J (2005) Nonlinear dynamical analysis of EEG and MEG: Review of an emerging field. Clin Neurophysiol. 116:2266–2301 DOI 10.1016/j.clinph.2005.06.011
[46] Varma N K, Kushwaha R, Beydoun A et al (1997) Mutual information analysis and detection of interictal morphological differences in interictal epileptiform discharges of patients with partial epilepsies. Electroenceph Clin Neurophysiol 103: 426–433. DOI 10.1016/S0013-4694(97)00039-4
[47] Vastano J A, Swinney H L (1988) Information transport in spatiotemporal systems. Phys Rev Lett 60:1773–1776 DOI 10.1103/PhysRevLett.60.1773
[48] Xu J, Liu Z R, Liu R et al (1997) Information transformation in human cerebral cortex. Physica D 106:363–374 DOI 10.1016/S0167-2789(97)00042-0
[49] Zhang X S, Roy R J (2001) Derived fuzzy knowledge model for estimating the depth of anesthesia. IEEE Trans Biomed Eng 48:312–323 DOI 10.1109/10.914794
[50] Zweig M H, Campbell G (1993) Receiver-Operating Characteristic (ROC) plots: a fundamental evaluation tool in clinical medicine. Clin Chem 39:561–577.

Electrode	Control subjects (mean ± SD)	AD patients (mean ± SD)	p
F3	0.7378 ± 0.1821	0.6288 ± 0.1181	0.1115
F4	0.7100 ± 0.2028	0.6933 ± 0.1371	0.8242
F7	0.7732 ± 0.2072	0.7349 ± 0.1634	0.6355
F8	0.7867 ± 0.1775	0.7309 ± 0.1563	0.4426
Fp1	0.7182 ± 0.1649	0.5641 ± 0.2006	0.0631
Fp2	0.6994 ± 0.2194	0.5745 ± 0.1363	0.1243
T3	0.9580 ± 0.2869	0.9236 ± 0.2472	0.7663
T4	0.9296 ± 0.2485	0.9342 ± 0.3186	0.9701
T5	0.9125 ± 0.1953	0.6936 ± 0.2081	0.0193
T6	0.8976 ± 0.2018	0.6914 ± 0.2179	0.0322
C3	0.8363 ± 0.1670	0.7291 ± 0.1954	0.1820
C4	0.8490 ± 0.1384	0.7703 ± 0.2150	0.3198
P3*	0.8599 ± 0.1331	0.6088 ± 0.1817	0.0014
P4*	0.8644 ± 0.1320	0.6423 ± 0.1753	0.0031
O1*	0.9714 ± 0.1801	0.6989 ± 0.1939	0.0027
O2*	0.9357 ± 0.2051	0.6867 ± 0.1961	0.0086

Table 1. Average $ApEn(m = 1, r = 0.25)$ for control subjects and AD patients in all channels. Results are shown as mean ± standard deviation (SD). Significant differences are marked with an asterisk.

Electrode	Control subjects (mean ± SD)	AD patients (mean ± SD)	*p*
F3	-32.22 ± 9.22	-25.30 ± 4.43	0.0363
F4	-32.56 ± 7.42	-27.36 ± 6.21	0.0894
F7	-32.35 ± 9.75	-29.76 ± 9.05	0.5244
F8	-34.13 ± 9.05	-29.95 ± 8.83	0.2855
Fp1	-32.11 ± 8.55	-23.26 ± 5.99	0.0108
Fp2	-30.39 ± 9.53	-21.74 ± 5.64	0.0174
T3	-38.78 ± 11.87	-37.43 ± 13.12	0.8029
T4	-38.32 ± 10.10	-38.89 ± 16.91	0.9247
T5*	-37.98 ± 8.99	-24.79 ± 7.48	0.0013
T6*	-37.09 ± 8.32	-26.59 ± 8.51	0.0084
C3	-35.60 ± 7.72	-30.67 ± 8.10	0.1595
C4	-36.48 ± 8.36	-32.34 ± 9.29	0.2856
P3*	-37.08 ± 7.26	-24.13 ± 6.91	0.0004
P4*	-37.52 ± 6.95	-25.55 ± 6.76	0.0006
O1*	-39.97 ± 8.83	-26.33 ± 8.33	0.0013
O2*	-37.33 ± 9.30	-25.99 ± 8.30	0.0068

Table 2. Average *AMI* rates of decrease for control subjects and AD patients in all channels. Results are shown as mean ± standard deviation (SD). Significant differences are marked with an asterisk.

Method	Electrode	Threshold	Sensitivity (%)	Specificity (%)	Accuracy (%)	AUC
ApEn(*m*=1, *r*=0.25)	P3	0.7326	72.73	81.82	77.27	0.8595
	P4	0.7381	63.64	81.82	72.73	0.8264
	O1	0.8181	81.82	72.73	77.27	0.8595
	O2	0.8190	90.91	63.64	77.27	0.7769
AMI rate of decrease	T5	-31.60	90.91	72.73	81.82	0.8678
	T6	-31.03	81.82	81.82	81.82	0.8512
	P3	-34.43	100.00	81.82	90.91	0.9339
	P4	-30.70	81.82	81.82	81.82	0.9091
	O1	-31.86	81.82	81.82	81.82	0.8678
	O2	-30.72	81.82	81.82	81.82	0.8264
SampEn(*m*=1, *r*=0.25)	P3	0.6658	72.73	81.82	77.27	0.8512
	P4	0.6740	63.64	90.91	77.27	0.8347
	O1	0.7492	81.82	72.73	77.27	0.8595
	O2	0.7367	90.91	63.64	77.27	0.7769
LZ complexity (3 symbol conversion)	T5	0.4161	72.73	72.73	72.73	0.8017
	P3	0.3962	81.82	81.82	81.82	0.8926
	P4	0.3485	72.73	90.91	81.82	0.8430
	O1	0.4412	90.91	72.73	81.82	0.8512
Slope of MSE(*m*=1, *r*=0.25, 12 scales) *for large time scales*	F3	-0.0037	81.82	81.82	81.82	0.8430
	F7	-0.0020	81.82	72.73	77.27	0.8347
	Fp1	-0.0026	90.91	90.91	90.91	0.9339
	Fp2	-0.0113	100	72.73	86.36	0.8512
	T5	-0.0167	90.91	81.82	86.36	0.9174
	T6	-0.0155	81.82	81.82	81.82	0.9008
	P3	-0.0119	81.82	90.91	86.36	0.9174
	P4	-0.0097	72.73	90.91	81.82	0.8512
	O1	-0.0116	81.82	90.91	86.36	0.9174
	O2	-0.0079	81.82	81.82	81.82	0.8760

AUC: Area under the ROC (Receiver Operating Characteristic) curve

Table 3. Test results for *ApEn*, the *AMI* rate of decrease, *SampEn*, *LZ* complexity and *MSE* on the channels in which the differences between both groups were significant. The optimum threshold to discriminate AD patients and control subjects and the area under the ROC curve are also included.

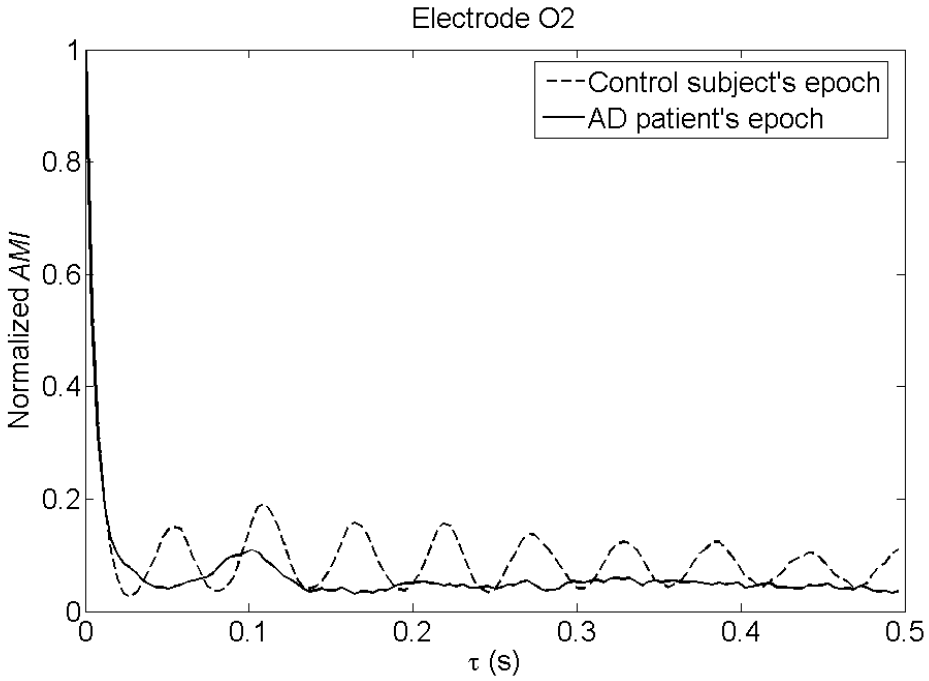

(a)

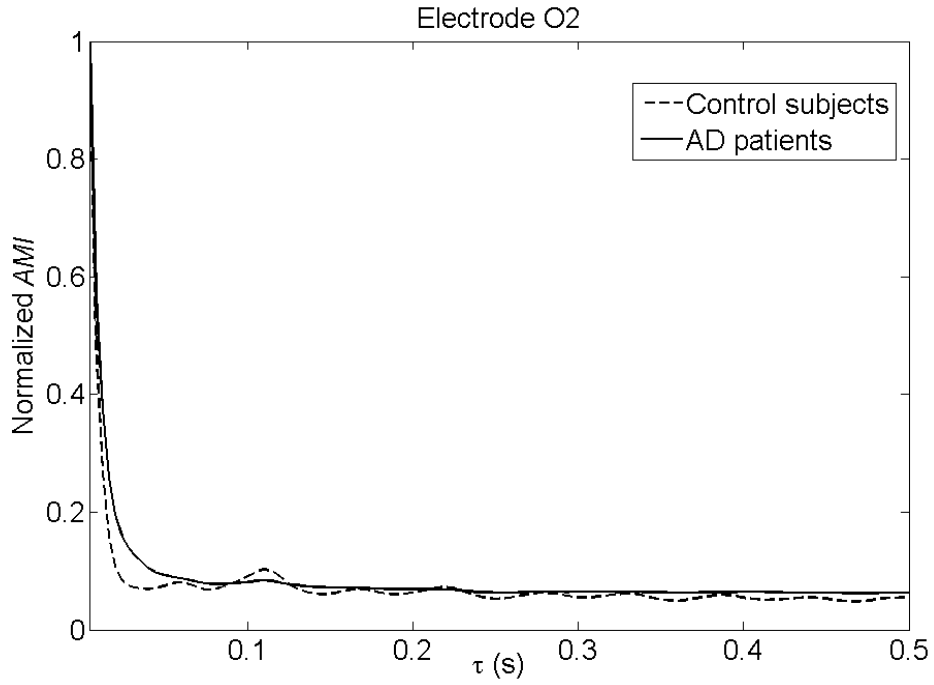

(b)

Figure 1. (a) Normalized *AMI* curves obtained from one AD patient's epoch and from a control subject's one. (b) Normalized *AMI* curves of the 11 control subjects and 11 AD patients at electrode O2.

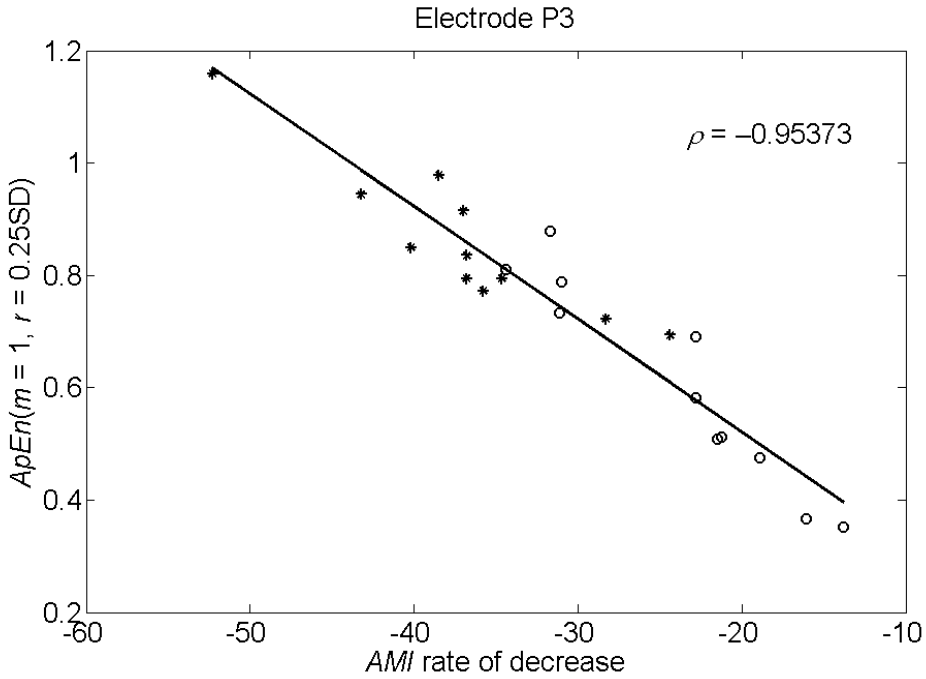

Figure 2. *ApEn* values versus the *AMI* rates of decrease for AD patients (circumferences) and control subjects (asterisks) at electrode P3. Pearson's correlation index is ρ = –0.95373. The straight line that fits the data in a least-squares sense has been plotted.